Check for updates

*CORRESPONDENCE
Guifu Wu
✉ wuguifu@mail.sysu.edu.cn
Yahui Zhang
✉ zyh1171518067@163.com

†These authors have contributed equally to this work

Enhanced external counterpulsation improves dysfunction of forearm muscle caused by radial artery occlusion

Zhenyu Wang[1†], Chun Yao[1†], Lihan Huang[1], Jianwen Liang[1], Xiaocong Zhang[2], Jian Shi[1], Wenbin Wei[1], Jing Zhou[3], Yahui Zhang[1,4]* and Guifu Wu[1,5,6]*

[1]Department of Cardiology, The Eighth Affiliated Hospital of Sun Yat-sen University, Shenzhen, Guangdong, China, [2]Department of Cardiology, Foshan Fosun Chancheng Hospital, Foshan, Guangdong, China, [3]Department of Cardiology, Affiliated Hospital of Yan'an University, Yan'an, Shaanxi, China, [4]School of Rehabilitation Sciences and Engineering, University of Health and Rehabilitation Sciences, Shandong, China, [5]Guangdong Innovative Engineering and Technology Research Center for Assisted Circulation, Sun Yat-sen University, Shenzhen, Guangdong, China, [6]NHC Key Laboratory of Assisted Circulation, Sun Yat-sen University, Guangzhou, Guangdong, China

Objective: This study aimed to investigate the therapeutic effect of enhanced external counterpulsation (EECP) on radial artery occlusion (RAO) through the oscillatory shear (OS) and pulsatile shear (PS) models of human umbilical vein endothelial cells (HUVECs) and RAO dog models.

Methods: We used high-throughput sequencing data GSE92506 in GEO database to conduct time-series analysis of functional molecules on OS intervened HUVECs, and then compared the different molecules and their functions between PS and OS. Additionally, we studied the effect of EECP on the radial artery hemodynamics in Labrador dogs through multi-channel physiological monitor. Finally, we studied the therapeutic effect of EECP on RAO at the histological level through Hematoxylin−Eosin staining, Masson staining, ATPase staining and immunofluorescence in nine Labrador dogs.

Results: With the extension of OS intervention, the cell cycle decreased, blood vessel endothelial cell proliferation and angiogenesis responses of HUVECs were down-regulated. By contrast, the inflammation and oxidative stress responses and the related pathways of anaerobic metabolism of HUVECs were up-regulated. Additionally, we found that compared with OS, PS can significantly up-regulate muscle synthesis, angiogenesis, and NO production related molecules. Meanwhile, PS can significantly down-regulate inflammation and oxidative stress related molecules. The invasive arterial pressure monitoring showed that 30Kpa EECP treatment could significantly increase the radial artery peak pressure (p =0.030, 95%CI, 7.236−82.524). Masson staining showed that RAO significantly increased muscle interstitial fibrosis (p =0.002, 95%CI, 0.748−2.128), and EECP treatment can reduce this change (p =0.011, 95%CI, −1.676 to −0.296). ATPase staining showed that RAO significantly increased the area of type II muscle fibers (p =0.004, 95%CI, 7.181−25.326), and EECP treatment could reduce this change (p =0.001, 95%CI, −29.213 to −11.069). In addition, immunofluorescence showed that EECP increased angiogenesis in muscle tissue (p =0.035, 95%CI, 0.024−0.528).

Conclusion: EECP improves interstitial fibrosis and hypoxia, and increases angiogenesis of muscle tissue around radial artery induced by RAO.

Introduction

In 1989, Campeau reported for the first time that it was conducted coronary angiography through transradial artery access (TRA) (1). The advantages of no braking after TRA operation contribute to improved patient comfort, reduced bleeding and hematoma, shortened hospital stay and reduced medical costs (2). In addition, TRA also reduced mortality in high-risk patient subgroups, such as those presenting with acute coronary syndromes (3, 4). In 2018, the European Society of Cardiology and the European Association of Cardiothoracic Surgery recommended TRA as a preferred approach for coronary artery diagnosis and treatment (5).

Radial artery occlusion (RAO) is the most frequent post-procedural complication of TRA. Several studies have demonstrated significant structural changes after TRA catheterization (6, 7). The primary mechanism of early RAO after TRA consists of acute arterial thrombosis, resulting from the combined effect of catheter-related endothelial and vessel injury, local hypercoagulable state, and decreased blood flow from compressive hemostasis (8). Most early RAO patients are missed due to radial artery palpation. Chronic RAO will account for a large proportion of these patients. It can be caused by the proliferation of vascular smooth muscle and the progressive thickening of the intima media caused by proliferation (6, 9). Several studies have shown that the expression of important active factors such as nitric oxide (NO) and vascular endothelial growth factor (VEGF) in vascular endothelial cells is decreased (10, 11), and the expression of inflammatory and procoagulant molecules nuclear factor-kappaB (NF-κB), Von Willebrand factor (vWF) and tissue factor (TF) is increased (8, 12, 13), which may be involved in the occurrence of RAO. Relative studies shows that RAO can be prevented effectively by adequate procedural anticoagulation (14, 15), proper transradial artery duration and magnitude of compression (16, 17), and reduction of sheath and catheter size (6, 18). However, the increase in the number of percutaneous coronary intervention and non-standard operations still result in a large number of RAO patients. Although asymptomatic from an ischemia standpoint in the vast majority of cases, it precludes ipsilateral TRA for future procedures. If there is symptomatic hand ischemia, it may be necessary to reopen an occluded radial artery for transradial procedure (19, 20). This will undoubtedly increase the related vascular complications again.

Oscillatory shear stress (OS) will be generated at the stenotic artery, which will lead to vascular dysfunction and atherosclerosis, and may further aggravate the degree of arterial stenosis (21). Conversely, physiologically high shear stress is protective, which can improve vascular endothelial function and reduce atherosclerosis. Among them, endothelial cells are critical sensors of shear stress (22). Enhanced external counterpulsation (EECP)is a non-invasive pneumatic technology. It can not only effectively increase diastolic blood pressure, mean coronary artery pressure and coronary artery flow, but also reduce main artery systolic blood pressure by controlling a series of lower limb cuffs to inflate in the diastole and deflate in the systole, generate characteristic double pulse blood flow. Our previous animal studies had demonstrated that EECP intervention could inhibit intimal hyperplasia, restore vascular endothelial function by increasing pulsatile shear (PS) stress and modifying shear stress responsive gene expression, attenuate atherosclerosis progression through modulation of proinflammatory pathway, as well as promote coronary collaterals and angiogenesis (13, 23–25).

As far as we know, there is no noninvasive treatment that can significantly improve RAO. In this study, we analyzed the transcriptome of human umbilical vein endothelial cells (HUVECs) from the longitudinal time series and horizontal comparison through the OS and PS model *in vitro*. Furthermore, we further studied the evidence that EECP can improve RAO at invasive hemodynamic and histological levels through animal experiments.

Materials and methods

High throughput sequencing data archives

The expression profiles by an array of GSE92506 were retrieved from GEO database. To profile shear stress-regulated endothelial transcriptomes, researchers performed RNA-seq with HUVECs subjected to different shear flow conditions, including atheroprotective PS (12 ± 4 dyn/cm^2) and atheroprone OS (0.5 ± 4 dyn/cm^2), or kept as static control for four time periods (1, 4, 12 and 24 h). The Platform of high throughput sequencing is GPL15433 (Illumina HiSeq 1000, Homo sapiens). Series matrix files and data table header descriptions of GSE92506 were downloaded from the GEO database to describe the change trend of differential molecules through transcriptome time-series analysis of OS intervention HUVECs. In addition, we have compared the differential molecules between PS and OS at 24 h.

Data transformations and differential molecular screening

We used the R package "DEseq2" (v3.6.3) to analyze the differentially expressed genes (DEG) between OS and ST at different time points (26), and found that the genes with p.adj < 0.05 and Log2 (Flod Change) > 1 or < −1 had significant differences. R package "Mfuzzy" (v2.20.0) was used to cluster the standardized high-throughput sequencing data of DEG (OS vs. Static) with fuzzy C-means to describe their changing trend over time. The minimum centroid distance of a series of clusters was calculated and classified into different clusters. In addition, we also analyzed the differences between OS and ST at 24 h, DEG was presented by volcano map.

Pathway enrichment and dynamic analysis

We used Gene Ontology/Kyoto Encyclopedia of Genes and Genomes (GO/KEGG) (27). The pathway with p.adj < 0.05 is considered to be significantly enriched. The direction of the pathway was calculated using the average value of the difference multiple of the important molecules (p.adj < 0.05) in the significantly enriched pathway. Compared with baseline, all significant mRNA were used as the background for pathway dynamic analysis (28).

Animals and groups

A total of 9 female Labrador dogs (24 weeks old, average weight 19 ± 0.4 kg) were purchased from Jinan Jinfeng Experimental Animal Co., Ltd. and raised in Shenzhen Leading Medical Service Co., Ltd. The

rearing environment: temperature (22–28°C), humidity (50–70%), density (2 dogs/cage), free drinking water, feeding (2 times/day), lighting time (07:30–19:30). The animals were randomly divided into three groups (each group $n = 3$): Control, RAO and RAO-EECP. The animal experiment part of this study has been approved by the Medical Research Ethics Committee of the Eighth Affiliated Hospital of Sun Yat-sen University (Futian, Shenzhen) (Research Ethics of the Eighth Affiliated Hospital of Sun Yat-sen University 2021-037-01).

Radial artery hemodynamic measurements

Hemodynamic parameters of the left radial artery during EECP intervention were measured in 3 dogs to determine the best counterpulsation pressure. Intramuscular injection of 0.5–1 mg/kg (Jilin Fanggong, China) of xylazine hydrochloride injection was used for induction anesthesia, followed by endotracheal intubation for ventilation (Mindray veta5, China). After that, isoflurane (Baxter Healthcare, United States) was used for continuous anesthesia to maintain SO_2 at 100%. The animal was then placed in supine position on the counter pulsation bed, and a set of modified dog-specific cuff was wrapped to closely fit the lower limbs and buttocks of the dog for EECP (PSK P-ECP/TM Oxygen Saturation Monitor, China). The cuff was inflated with compressed air from the distal end to the proximal end successively in early diastole, and deflated rapidly before systole of the next cardiac cycle. The invasive arterial pressure of the left radial artery was monitored with a multi-channel physiological monitor (BIOPAC, MP150) to evaluate the appropriate counterpulsation pressure for EECP treatment.

RAO model and EECP treatment

The left radial artery of 6 dogs was ligated, and the RAO-EECP group was performed 30Kpa EECP for 60 min every day within 14 days. In order to eliminate possible circadian influence, EECP were conducted at the same time of every day.

Tissue preparation

All dogs were anesthetized with xylazine hydrochloride injection (Jilin Fanggong, China), at the same time, all animals were euthanized by intravenous injection of excessive 10% potassium chloride at the same time as well. At the end of the experiment, the lateral muscle samples of left forearm of all dogs were taken immediately and washed in cold normal saline. The sample of each dog was divided into four parts, which were fixed with 4% paraformaldehyde and then embedded in paraffin for HE staining and collagen staining, embedded with OCT embedding agent (SAKURA, Japan) and frozen in liquid nitrogen for ATPase staining (29). In addition, another 4% paraformaldehyde samples were used for immunofluorescence.

Morphological evaluation

The detailed experimental protocol of Hematoxylin–Eosin staining, Masson staining, ATPase staining and immunofluorescence are showed in the Supplemental material.

Statistical analysis

We conducted Shapiro Wilk normality test for all quantitative data. For normal distribution samples, Student's t-tests and ANOVA were used to compare parameter data between two conditions and multiple conditions, respectively. The homogeneity of variance was evaluated by Levene's test. For ANOVA analysis, multiple hypothesis test (Tukey HSD test) was used and corrected by Bonferroni method. In addition, we used the R package "ggplot2" (v3.3.3) and GraphPad Prism (v9.1.1) to visualize the above statistical analysis data.

Results

Time-series mRNA expression and pathway dynamic enrichment analysis

The important molecules (p.adj < 0.05) at each time point compared with static under OS intervention were divided into four main longitudinal trajectories by C-means clustering (Figure 1A) according to their expression trend. We can find that the expression of molecules in Cluster 1, 2 and 3 reached the peak at 1 h, and then the expression of molecules in Cluster 1 decreased rapidly at 4 h, and then slowly recovered, while the expression of molecules in Cluster 2 and 3 decreased slowly after 1 h until 24 h. On the contrary, the molecular expression in Cluster 4 was gradually up-regulated until it reached peak at 12 h.
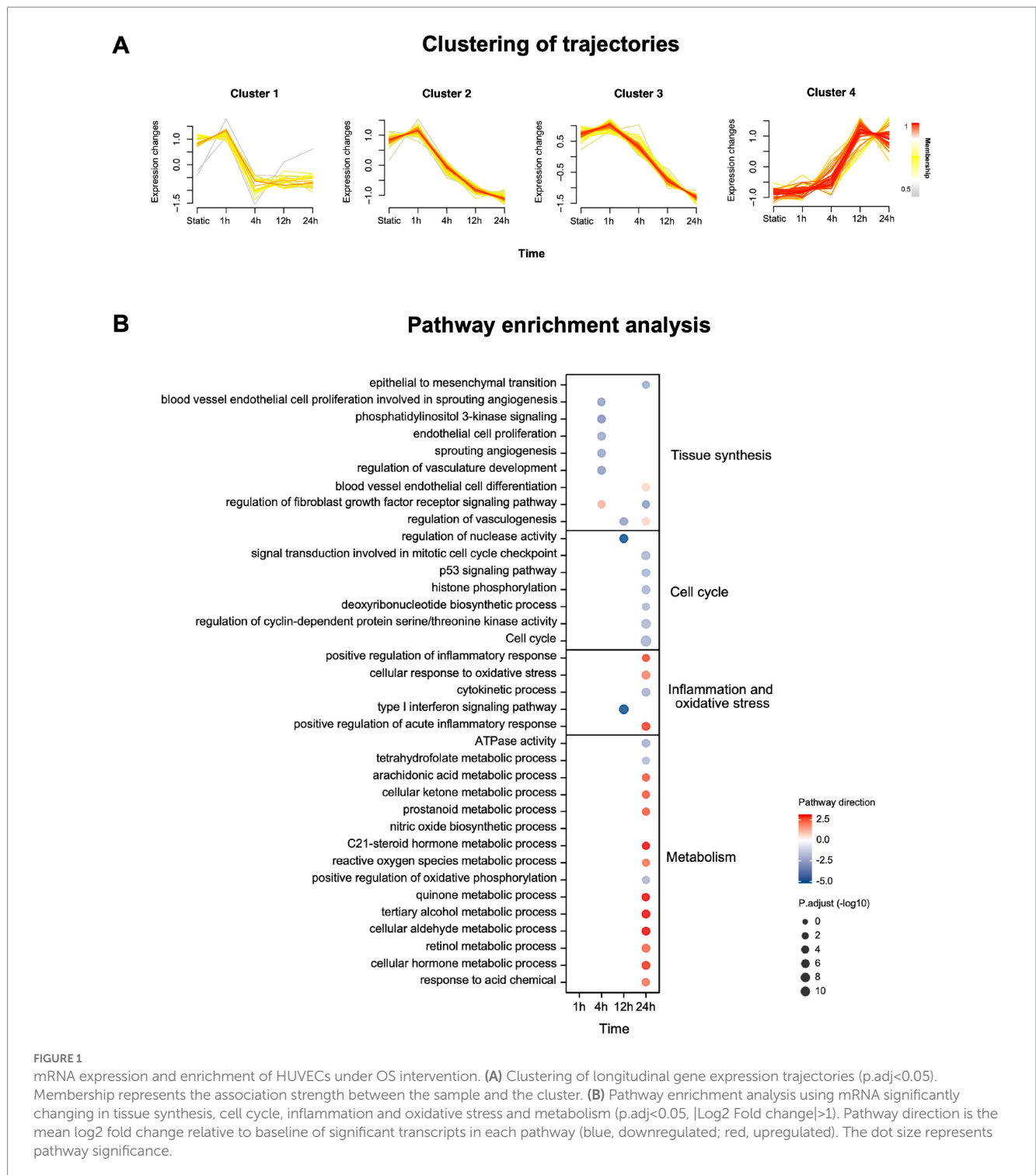
At each time point, we use all important mRNA (p.adj < 0.05) to conduct enrichment analysis on dynamic pathways related to tissue synthesis, cell cycle, inflation and oxidative stress and metabolism (Figure 1B). The results showed that with the extension of OS intervention, the cell cycle decreased, blood vessel endothelial cell proliferation and angiogenesis responses were down-regulated. By contrast, the inflammation and oxidative stress responses and the related pathways of anaerobic metabolism of HUVECs were up-regulated. The details of time-series mRNA expression and pathway dynamic enrichment analysis were in Supplementary data sheet.

Horizontal comparative analysis

We performed a differential analysis on mRNA of HUVECs after 24 h PS and OS intervention (Figure 2). We found that compared with OS, PS can significantly up-regulate muscle synthesis related molecules (such as *GLI1*, *TGM2*, *SULF1*, etc.) (30–35), angiogenesis related molecules (such as *CD34*, *CYP1B1*, *AQP1*, *ECM1*, *GPER1*, *HMOX1*, *RAMP2*, etc.) (36–48), and NO production related molecules (such as *ASS1*, *GCH1*, *NOS3*, *KLF4*, *KLF2*, etc.) (49–56). In addition, PS can significantly down-regulate inflammation and oxidative stress related molecules (such as *IL7*, *INHBA*, *CCL7*, *CXCL12*, *TGFBR1*, *CXCR4*, *IL1RL1*, *TNFSF15*, *ITGA4*, etc.) (57–72).

Radial artery hemodynamic measurements

Multi-channel physiological monitor shows the arterial flow and pressure in multiple parts of the body, including invasive radial artery pressure, under the intervention of different counterpulsation pressures (Figure 3A). We found that EECP can produce characteristic

FIGURE 1
mRNA expression and enrichment of HUVECs under OS intervention. **(A)** Clustering of longitudinal gene expression trajectories (p.adj<0.05). Membership represents the association strength between the sample and the cluster. **(B)** Pathway enrichment analysis using mRNA significantly changing in tissue synthesis, cell cycle, inflammation and oxidative stress and metabolism (p.adj<0.05, |Log2 Fold change|>1). Pathway direction is the mean log2 fold change relative to baseline of significant transcripts in each pathway (blue, downregulated; red, upregulated). The dot size represents pathway significance.
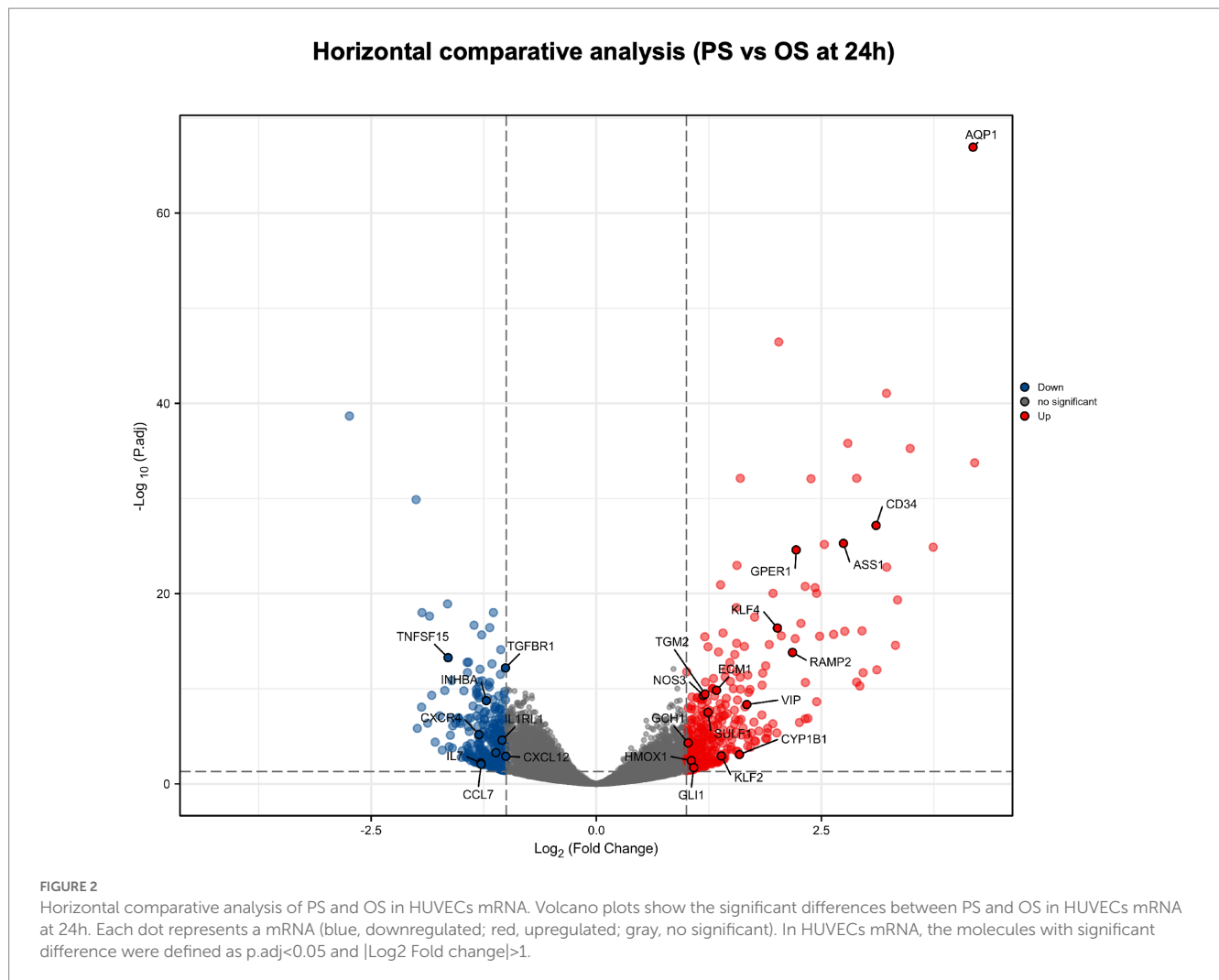
double pulse blood flow, and the radial artery peak pressure is the highest under the intervention of 30Kpa counterpulsation pressure ($p = 0.030$, 95%CI, 7.236 to 82.524). We took 30Kpa as the subsequent counterpulsation pressure parameter (Figure 3B).

Morphological evaluation

In accordance with the predetermined research protocol (Figure 4A), we completed the establishment of the Labrador dog's RAO model, the EECP treatment, the collection of skeletal muscle

samples and related tests. The pathological staining results showed that (Figure 4B), there was no significant difference in the Hematoxylin eosin staining of the lateral muscle of left forearm among the three groups. However, Masson staining showed that the interstitial fibrosis of lateral muscle of left forearm caused by RAO ($p = 0.002$, 95%CI, 0.748–2.128), while after the treatment of EECP, the interstitial fibrosis was significantly reduced ($p = 0.011$, 95%CI, −1.676 to −0.296, Figure 4C). ATPase staining showed that type II muscle fibers in RAO group were significantly increased compared with control group ($p = 0.004$, 95%CI, 7.181–25.326), while type II muscle fibers were significantly decreased after treatment with EECP ($p = 0.001$, 95%CI,

FIGURE 2
Horizontal comparative analysis of PS and OS in HUVECs mRNA. Volcano plots show the significant differences between PS and OS in HUVECs mRNA at 24h. Each dot represents a mRNA (blue, downregulated; red, upregulated; gray, no significant). In HUVECs mRNA, the molecules with significant difference were defined as p.adj<0.05 and |Log2 Fold change|>1.

−29.213 to −11.069, Figure 4D). Immunofluorescence showed that the expression of VWF was significantly up-regulated in lateral muscle of left forearm after treatment with EECP ($p = 0.035$, 95%CI, 0.024–0.528, Figure 4E), which proved that EECP increased angiogenesis.

Discussion

The real-world reported incidence of RAO remains the most frequent postprocedural complication of transradial access, with limited choice in the uptake of RAO therapeutic strategies. The reduction of sheath and catheter size (18), use of intraprocedural heparin (14), and maintenance of radial artery patency during hemostasis and oral anticoagulation (16) after TRA have been shown to lower the risk of RAO and have been termed best practices. Recently, The PROPHET-II Randomized Trial showed that prophylactic ipsilateral ulnar artery compression during radial artery hemostasis could significantly reduce the risk of RAO at the time of 24 h and 30 days after the procedure (73). However, there is no dedicated devices capable of dual compression on the market at present, which poses a great challenge for the wide application. In addition, recanalization of the occluded radial artery *via* the distal radial access (DRA) was reproted to be safe and effective, but the available evidence remains currently limited (74).

OS will be produced at the artery stenosis site, which further will lead to vascular dysfunction and atherosclerosis (21). In this study, we used the OS and PS models of HUVECs to analyze the longitudinal time-series of HUVECs mRNA. We finally found that with the prolongation of OS intervention, cell cycle, and vascular endothelial cell proliferation and angiogenesis response were down-regulated. At the same time, the inflammatory and oxidative stress responses and the related pathways of anaerobic metabolism of HUVEC were up-regulated. In addition, we found that PS intervention can significantly up-regulate the muscle synthesis, angiogenesis and NO production related molecules of HUVECs relative to OS, and significantly down-regulate the Inflammation and oxidative stress related molecules. This phenomenon may explain why arterial stenosis is aggravated, and the importance of PS for maintaining vascular function.

Our previous studies showed that EECP intervention can produce characteristic double pulse blood flow, and endothelial protective laminar flow to coronary artery, so as to restore vascular endothelial function by increasing pulsating shear stress and changing the expression of shear stress response gene, slow down the progress of atherosclerosis by regulating the proinflammatory pathway, and promote coronary collateral and angiogenesis (13, 23–25). However, there is no relevant research to prove whether EECP can produce similar blood flow pattern and function to coronary artery for radial artery.
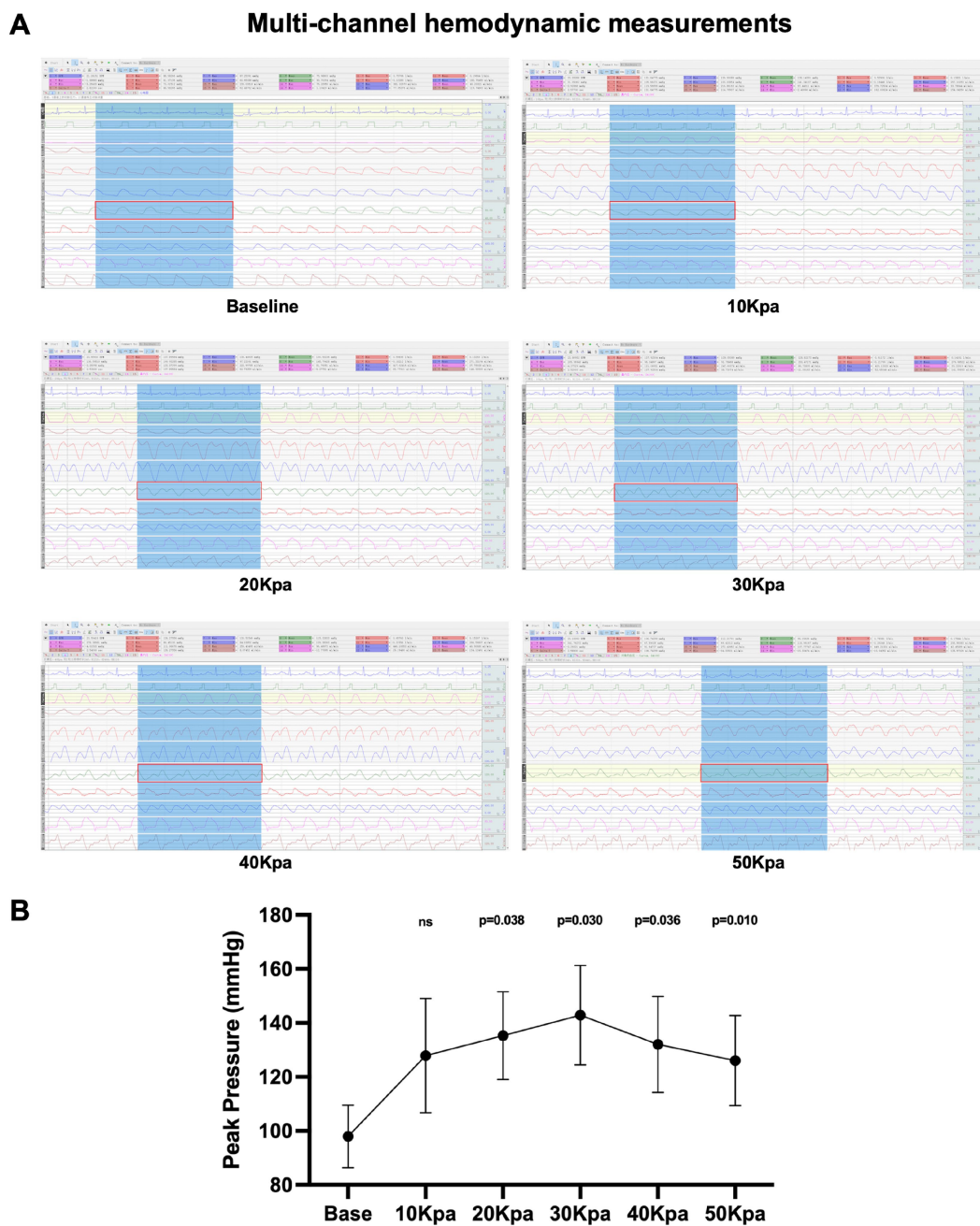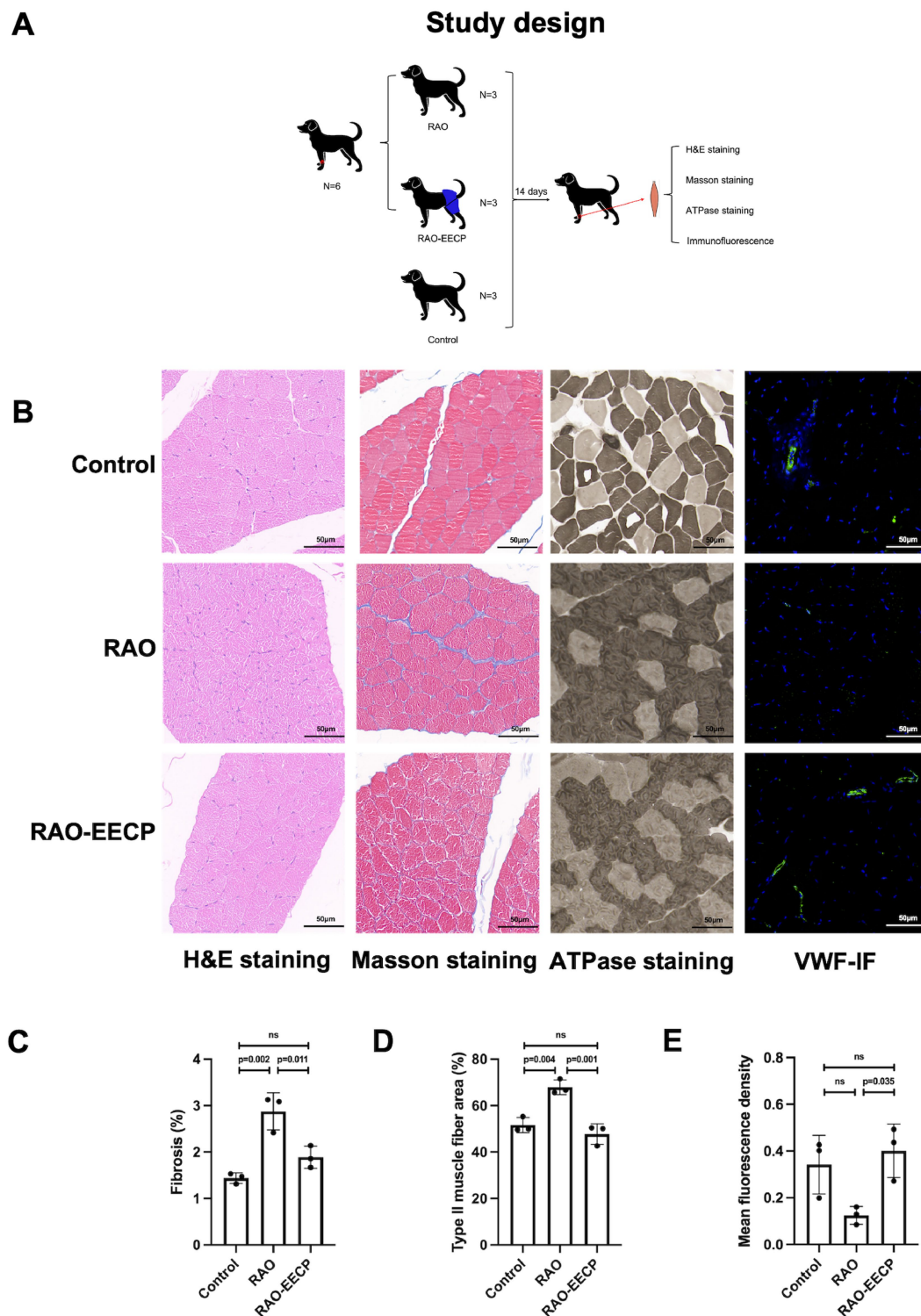
FIGURE 3

Multi-channel hydrodynamic measurements under EECP intervention. **(A)** Multi-channel hydrodynamic measurements of different counterpulsation pressures. The eighth channel (red rectangle) is the radial artery pressure. **(B)** Peak pressure of radial artery under different counterpulsation pressure. Data were expressed as means$\pm$SD (n =3). Results were evaluated by Student's t-test (each counterpulsation pressure with baseline).

In this study, we first evaluated the hemodynamic changes of the radial artery under the intervention of EECP through invasive radial artery pressure monitoring. We also found that the most appropriate counterpulsation pressure was 30Kpa. According to Hagen Poiseuille and Navier Stokes formulas (75), blood viscosity and the diameter of the vascular cavity remain unchanged, and the pressure gradient is proportional to the shear stress. We prove that EECP can generate double pulse blood flow and significantly increase the blood flow shear stress.

After that, we artificially made the local OS of the radial artery through the RAO model of Labrador dogs, and observed the histological changes of the muscle around the radial artery. At the same time, we used the EECP protocol (30Kpa, 1 h/day) to treat other RAO dogs for 14 days. The results showed that H&E staining had no serious muscle damage in the three groups, but Masson staining showed that RAO might cause interstitial fibrosis in local muscles, indicating that RAO may cause certain inflammatory reaction to surrounding muscle tissue, and muscle interstitial fibrosis was significantly reduced after treatment with EECP. In addition, ATPase staining demonstrated that RAO may cause a significant increase of type II muscle fibers in local muscle tissue, while type II muscle fibers are significantly reduced and type I muscle fibers are significantly increased after treatment with EECP. Researches showed that type II

FIGURE 4
EECP promotes angiogenesis, improves muscle damage and aerobic metabolism. **(A)** Animal study design. **(B)** From left to right: H&E staining, Masson staining, ATPase staining and VWF immunofluorescence (IF) of cross section of lateral muscle of left forearm of Labrador dogs in three groups. Scale bars, 50μm. There was no significant difference in H&E staining among the three groups. VWF, Von Willebrand Factor. **(C)** Quantification of fibrotic regions (appearing as blue in Masson's trichome in **C**). Data were expressed as means±SD (n =3 per group). Results were evaluated by one-way ANOVA followed by Tukey HSD test. **(D)** Quantification of type II muscle fibers (appearing as dark grey in **B**). Data were expressed as means±SD (n =3 per group). Results were evaluated by one-way ANOVA followed by Tukey HSD test. **(E)** Quantification of VWF immunofluorescence. Data were expressed as means±SD (n =3 per group). Results were evaluated by one-way ANOVA followed by Tukey HSD test.

muscle fibers are mainly responsible for anaerobic metabolism, while type I muscle fibers are mainly responsible for aerobic metabolism (76). Therefore, we judged that RAO may cause insufficient local

perfusion, leading to ischemia and hypoxia of muscle tissue, and EECP may improve this pathological state. Finally, we evaluated angiogenesis through the vascular marker VWF. The IF results showed that EECP

may significantly increase angiogenesis in the local muscle tissue of the radial artery.

Limitations and future research

Our research also has some limitations. There are some differences between the potential causes of RAO in clinical patients and the RAO animal model in this study, including the atherosclerosis, vascular access, artistic cather, exposure to wires, etc. Therefore, the results of this study cannot fully reflect the clinical efficacy of EECP on RAO. In addition, we have only verified in animal tests that the pulsating shear stress generated by EECP, and have not further performed clinical verification on patients with RAO stenosis. We will further conduct a multicenter randomized controlled trial to further verify the benefits of EECP for RAO patients.

Conclusion

EECP can produce characteristic double pulse blood flow shear stress, and the radial artery peak pressure reaches the highest under the action of 30Kpa counterpulsation pressure. In addition, EECP may improve RAO induced interstitial fibrosis and hypoxia of muscle tissue around the radial artery, and increase angiogenesis of muscle tissue around the radial artery.

Data availability statement

The datasets presented in this study can be found in online repositories. The names of the repository/repositories and accession number(s) can be found in the article/Supplementary material.

Ethics statement

The animal study was reviewed and approved by Medical Research Ethics Committee of the Eighth Affiliated Hospital of Sun Yat-sen University (Futian, Shenzhen) and affiliated to the Eighth Affiliated Hospital of Sun Yat-sen University (Futian, Shenzhen).

Author contributions

ZW and GW proposed the scientific problems. ZW and CY designed the experiments. ZW and JZ processed bioinformatics analysis. ZW, JL, XZ, JS, and WW processed and collected the animal experimental data. ZW and CY processed and calculated. All authors contributed to the article and approved the submitted version.

Conflict of interest

The authors declare that the research was conducted in the absence of any commercial or financial relationships that could be construed as a potential conflict of interest.

Publisher's note

All claims expressed in this article are solely those of the authors and do not necessarily represent those of their affiliated organizations, or those of the publisher, the editors and the reviewers. Any product that may be evaluated in this article, or claim that may be made by its manufacturer, is not guaranteed or endorsed by the publisher.

Supplementary material

The Supplementary material for this article can be found online at: https://www.frontiersin.org/articles/10.3389/fcvm.2023.1115494/full#supplementary-material

References

1. Campeau, L. Percutaneous radial artery approach for coronary angiography. *Catheter Cardiovasc Diagn*. (1989) 16:3–7. doi: 10.1002/ccd.1810160103

2. Feldman, DN, Swaminathan, RV, Kaltenbach, LA, Baklanov, DV, Kim, LK, Wong, SC, et al. Adoption of radial access and comparison of outcomes to femoral access in percutaneous coronary intervention: an updated report from the national cardiovascular data registry (2007-2012). *Circulation*. (2013) 127:2295–306. doi: 10.1161/CIRCULATIONAHA.112.000536

3. Valgimigli, M, Frigoli, E, Leonardi, S, Vranckx, P, Rothenbuhler, M, Tebaldi, M, et al. Radial versus femoral access and bivalirudin versus unfractionated heparin in invasively managed patients with acute coronary syndrome (MATRIX): final 1-year results of a multicentre, randomised controlled trial. *Lancet*. (2018) 392:835–48. doi: 10.1016/S0140-6736(18)31714-8

4. Ferrante, G, Rao, SV, Juni, P, Da Costa, BR, Reimers, B, Condorelli, G, et al. Radial versus femoral access for coronary interventions across the entire Spectrum of patients with coronary artery disease: a meta-analysis of randomized trials. *JACC Cardiovasc Interv*. (2016) 9:1419–34. doi: 10.1016/j.jcin.2016.04.014

5. Neumann, FJ, Sousa-Uva, M, Ahlsson, A, Alfonso, F, Banning, AP, Benedetto, U, et al. 2018 ESC/EACTS Guidelines on myocardial revascularization. *Eur Heart J*. (2019) 40:87–165. doi: 10.1093/eurheartj/ehy394

6. Yonetsu, T, Kakuta, T, Lee, T, Takayama, K, Kakita, K, Iwamoto, T, et al. Assessment of acute injuries and chronic intimal thickening of the radial artery after transradial coronary intervention by optical coherence tomography. *Eur Heart J*. (2010) 31:1608–15. doi: 10.1093/eurheartj/ehq102

7. Staniloae, CS, Mody, KP, Sanghvi, K, Mindrescu, C, Coppola, JT, Antonescu, CR, et al. Histopathologic changes of the radial artery wall secondary to transradial catheterization. *Vasc Health Risk Manag*. (2009) 5:527–32. doi: 10.2147/vhrm.s5468

8. Mamas, MA, Fraser, DG, Ratib, K, Fath-Ordoubadi, F, El-Omar, M, Nolan, J, et al. Minimising radial injury: prevention is better than cure. *EuroIntervention*. (2014) 10:824–32. doi: 10.4244/EIJV10I7A142

9. Abdelaal, E, Molin, P, Plourde, G, Machaalany, J, Bataille, Y, Brousseau-Provencher, C, et al. Successive transradial access for coronary procedures: experience of Quebec heart-lung institute. *Am Heart J*. (2013) 165:325–31. doi: 10.1016/j.ahj.2012.10.016

10. Heiss, C, Balzer, J, Hauffe, T, Hamada, S, Stegemann, E, Koeppel, T, et al. Vascular dysfunction of brachial artery after transradial access for coronary catheterization: impact of smoking and catheter changes. *JACC Cardiovasc Interv*. (2009) 2:1067–73. doi: 10.1016/j.jcin.2009.09.010

11. Hutter, R, Carrick, FE, Valdiviezo, C, Wolinsky, C, Rudge, JS, Wiegand, SJ, et al. Vascular endothelial growth factor regulates reendothelialization and neointima formation in a mouse model of arterial injury. *Circulation*. (2004) 110:2430–5. doi: 10.1161/01.CIR.0000145120.37891.8A

12. Mehrhof, FB, Schmidt-Ullrich, R, Dietz, R, and Scheidereit, C. Regulation of vascular smooth muscle cell proliferation: role of NF-kappaB revisited. *Circ Res*. (2005) 96:958–64. doi: 10.1161/01.RES.0000166924.31219.49

13. Wu, G, Du, Z, Hu, C, Zheng, Z, Zhan, C, Ma, H, et al. Angiogenic effects of long-term enhanced external counterpulsation in a dog model of myocardial infarction. *Am J Physiol Heart Circ Physiol*. (2006) 290:H248–54. doi: 10.1152/ajpheart.01225.2004

14. Hahalis, GN, Leopoulou, M, Tsigkas, G, Xanthopoulou, I, Patsilinakos, S, Patsourakos, NG, et al. Multicenter randomized evaluation of high versus standard heparin dose on incident radial arterial occlusion after Transradial coronary angiography: the SPIRIT OF ARTEMIS study. *JACC Cardiovasc Interv*. (2018) 11:2241–50. doi: 10.1016/j.jcin.2018.08.009

15. Pancholy, SB. Comparison of the effect of intra-arterial versus intravenous heparin on radial artery occlusion after transradial catheterization. *Am J Cardiol*. (2009) 104:1083–5. doi: 10.1016/j.amjcard.2009.05.057

16. Dangoisse, V, Guedes, A, Chenu, P, Hanet, C, Albert, C, Robin, V, et al. Usefulness of a gentle and short hemostasis using the Transradial band device after Transradial access for percutaneous coronary angiography and interventions to reduce the radial artery occlusion rate (from the prospective and randomized CRASOC I, II, and III studies). *Am J Cardiol*. (2017) 120:374–9. doi: 10.1016/j.amjcard.2017.04.037

17. Pancholy, SB, Heck, LA, and Patel, T. Forearm arterial anatomy and flow characteristics: a prospective observational study. *J Invasive Cardiol*. (2015) 27:218–21.

18. Rashid, M, Kwok, CS, Pancholy, S, Chugh, S, Kedev, SA, Bernat, I, et al. Radial artery occlusion after transradial interventions: a systematic review and meta-analysis. *J Am Heart Assoc*. (2016) 5:1–22. doi: 10.1161/JAHA.115.002686

19. Pancholy, SB. Transradial access in an occluded radial artery: new technique. *J Invasive Cardiol*. (2007) 19:541–4.

20. Babunashvili, A, and Dundua, D. Recanalization and reuse of early occluded radial artery within 6 days after previous transradial diagnostic procedure. *Catheter Cardiovasc Interv*. (2011) 77:530–6. doi: 10.1002/ccd.22846

21. Barber, T. Wall shear stress and near-wall flows in the stenosed femoral artery. *Comput Methods Biomech Biomed Engin*. (2017) 20:1048–55. doi: 10.1080/10255842.2017.1331342

22. Souilhol, C, Serbanovic-Canic, J, Fragiadaki, M, Chico, TJ, Ridger, V, Roddie, H, et al. Endothelial responses to shear stress in atherosclerosis: a novel role for developmental genes. *Nat Rev Cardiol*. (2020) 17:52–63. doi: 10.1038/s41569-019-0239-5

23. Luo, JY, Wu, GF, Xiong, Y, Chen, GW, Xie, Q, Yang, DY, et al. Enhanced external counterpulsation promotes growth cytokines-mediated myocardial angiogenesis in a porcine model of hypercholesterolemia. *Chin Med J*. (2009) 122:1188–94. doi: 10.3760/cma.j.issn.0366-6999.2009.10.014

24. Zhang, Y, He, X, Chen, X, Ma, H, Liu, D, Luo, J, et al. Enhanced external counterpulsation inhibits intimal hyperplasia by modifying shear stress responsive gene expression in hypercholesterolemic pigs. *Circulation*. (2007) 116:526–34. doi: 10.1161/CIRCULATIONAHA.106.647248

25. Zhang, Y, He, X, Liu, D, Wu, G, Chen, X, Ma, H, et al. Enhanced external counterpulsation attenuates atherosclerosis progression through modulation of proinflammatory signal pathway. *Arterioscler Thromb Vasc Biol*. (2010) 30:773–80. doi: 10.1161/ATVBAHA.109.197806

26. Love, MI, Huber, W, and Anders, S. Moderated estimation of fold change and dispersion for RNA-seq data with DESeq2. *Genome Biol*. (2014) 15:550. doi: 10.1186/s13059-014-0550-8

27. Yu, G, Wang, LG, Han, Y, and He, QY. clusterProfiler: an R package for comparing biological themes among gene clusters. *OMICS*. (2012) 16:284–7. doi: 10.1089/omi.2011.0118

28. Contrepois, K, Wu, S, Moneghetti, KJ, Hornburg, D, Ahadi, S, Tsai, MS, et al. Molecular choreography of acute exercise. *Cells*. (2020) 181:1112–1130.e16. doi: 10.1016/j.cell.2020.04.043

29. Hintz, CS, Coyle, EF, Kaiser, KK, Chi, MM, and Lowry, OH. Comparison of muscle fiber typing by quantitative enzyme assays and by myosin ATPase staining. *J Histochem Cytochem*. (1984) 32:655–60. doi: 10.1177/32.6.6202737

30. Yao, L, Tichy, ED, Zhong, L, Mohanty, S, Wang, L, Ai, E, et al. Gli1 defines a subset of fibro-adipogenic progenitors that promote skeletal muscle regeneration with less fat accumulation. *J Bone Miner Res*. (2021) 36:1159–73. doi: 10.1002/jbmr.4265

31. Pucci, S, Greggi, C, Polidoro, C, Piro, MC, Celi, M, Feola, M, et al. Clusterin silencing restores myoblasts viability and down modulates the inflammatory process in osteoporotic disease. *J Transl Med*. (2019) 17:118. doi: 10.1186/s12967-019-1868-5

32. Tran, TH, Shi, X, Zaia, J, and Ai, X. Heparan sulfate 6-O-endosulfatases (Sulfs) coordinate the Wnt signaling pathways to regulate myoblast fusion during skeletal muscle regeneration. *J Biol Chem*. (2012) 287:32651–64. doi: 10.1074/jbc.M112.353243

33. Piccioni, A, Gaetani, E, Neri, V, Gatto, I, Palladino, M, Silver, M, et al. Sonic hedgehog therapy in a mouse model of age-associated impairment of skeletal muscle regeneration. *J Gerontol A Biol Sci Med Sci*. (2014) 69:245–52. doi: 10.1093/gerona/glt076

34. Ribeiro, S, Ribeiro, C, Martins, VM, Honore, B, Neves-Petersen, MT, Gomes, AC, et al. Understanding myoblast differentiation pathways when cultured on Electroactive scaffolds through proteomic analysis. *ACS Appl Mater Interfaces*. (2022) 14:26180–93. doi: 10.1021/acsami.2c03444

35. Gill, R, Hitchins, L, Fletcher, F, and Dhoot, GK. Sulf1A and HGF regulate satellite-cell growth. *J Cell Sci*. (2010) 123:1873–83. doi: 10.1242/jcs.061242

36. Asahara, T, Murohara, T, Sullivan, A, Silver, M, van der Zee, R, Li, T, et al. Isolation of putative progenitor endothelial cells for angiogenesis. *Science*. (1997) 275:964–6. doi: 10.1126/science.275.5302.964

37. Verkman, AS. Aquaporins in endothelia. *Kidney Int*. (2006) 69:1120–3. doi: 10.1038/sj.ki.5000226

38. Ichikawa-Shindo, Y, Sakurai, T, Kamiyoshi, A, Kawate, H, Iinuma, N, Yoshizawa, T, et al. The GPCR modulator protein RAMP2 is essential for angiogenesis and vascular integrity. *J Clin Invest*. (2008) 118:29–39. doi: 10.1172/JCI33022

39. Sercu, S, Lambeir, AM, Steenackers, E, El Ghalbzouri, A, Geentjens, K, Sasaki, T, et al. ECM1 interacts with fibulin-3 and the beta 3 chain of laminin 332 through its serum albumin subdomain-like 2 domain. *Matrix Biol*. (2009) 28:160–9. doi: 10.1016/j.matbio.2009.02.003

40. Tang, Y, Scheef, EA, Gurel, Z, Sorenson, CM, Jefcoate, CR, and Sheibani, N. CYP1B1 and endothelial nitric oxide synthase combine to sustain proangiogenic functions of endothelial cells under hyperoxic stress. *Am J Physiol Cell Physiol*. (2010) 298:C665–78. doi: 10.1152/ajpcell.00153.2009

41. Ayer, A, Zarjou, A, Agarwal, A, and Stocker, R. Heme oxygenases in cardiovascular health and disease. *Physiol Rev*. (2016) 96:1449–508. doi: 10.1152/physrev.00003.2016

42. Trenti, A, Tedesco, S, Boscaro, C, Trevisi, L, Bolego, C, and Cignarella, A. Estrogen, angiogenesis, immunity and cell metabolism: solving the puzzle. *Int J Mol Sci*. (2018) 19:1–16. doi: 10.3390/ijms19030859

43. Mongiat, M, Fu, J, Oldershaw, R, Greenhalgh, R, Gown, AM, and Iozzo, RV. Perlecan protein core interacts with extracellular matrix protein 1 (ECM1), a glycoprotein involved in bone formation and angiogenesis. *J Biol Chem*. (2003) 278:17491–9. doi: 10.1074/jbc.M210529200

44. Fernandez-Sauze, S, Delfino, C, Mabrouk, K, Dussert, C, Chinot, O, Martin, PM, et al. Effects of adrenomedullin on endothelial cells in the multistep process of angiogenesis: involvement of CRLR/RAMP2 and CRLR/RAMP3 receptors. *Int J Cancer*. (2004) 108:797–804. doi: 10.1002/ijc.11663

45. Palenski, TL, Gurel, Z, Sorenson, CM, Hankenson, KD, and Sheibani, N. Cyp1B1 expression promotes angiogenesis by suppressing NF-kappaB activity. *Am J Physiol Cell Physiol*. (2013) 305:C1170–84. doi: 10.1152/ajpcell.00139.2013

46. Trenti, A, Tedesco, S, Boscaro, C, Ferri, N, Cignarella, A, Trevisi, L, et al. The glycolytic enzyme PFKFB3 is involved in estrogen-mediated angiogenesis via GPER1. *J Pharmacol Exp Ther*. (2017) 361:398–407. doi: 10.1124/jpet.116.238212

47. Skora, JP, Antkiewicz, M, Kupczynska, D, Kulikowska, K, Strzelec, B, Janczak, D, et al. Local intramuscular administration of ANG1 and VEGF genes using plasmid vectors mobilizes CD34+ cells to peripheral tissues and promotes angiogenesis in an animal model. *Biomed Pharmacother*. (2021) 143:112186. doi: 10.1016/j.biopha.2021.112186

48. Avolio, E, Katare, R, Thomas, AC, Caporali, A, Schwenke, D, Carrabba, M, et al. Cardiac pericyte reprogramming by MEK inhibition promotes arteriologenesis and angiogenesis of the ischemic heart. *J Clin Invest*. (2022) 132:1–17. doi: 10.1172/JCI152308

49. Mun, GI, Kim, IS, Lee, BH, and Boo, YC. Endothelial argininosuccinate synthetase 1 regulates nitric oxide production and monocyte adhesion under static and laminar shear stress conditions. *J Biol Chem*. (2011) 286:2536–42. doi: 10.1074/jbc.M110.180489

50. Douglas, G, Hale, AB, Patel, J, Chuaiphichai, S, Al Haj Zen, A, Rashbrook, VS, et al. Roles for endothelial cell and macrophage Gch1 and tetrahydrobiopterin in atherosclerosis progression. *Cardiovasc Res*. (2018) 114:1385–99. doi: 10.1093/cvr/cvy078

51. Lopez-Ramirez, MA, Lai, CC, Soliman, SI, Hale, P, Pham, A, Estrada, EJ, et al. Astrocytes propel neurovascular dysfunction during cerebral cavernous malformation lesion formation. *J Clin Invest*. (2021) 131:1–15. doi: 10.1172/JCI139570

52. Oliveira-Paula, GH, Lacchini, R, and Tanus-Santos, JE. Endothelial nitric oxide synthase: from biochemistry and gene structure to clinical implications of NOS3 polymorphisms. *Gene*. (2016) 575:584–99. doi: 10.1016/j.gene.2015.09.061

53. Morris, G, Puri, BK, Olive, L, Carvalho, A, Berk, M, Walder, K, et al. Endothelial dysfunction in neuroprogressive disorders-causes and suggested treatments. *BMC Med*. (2020) 18:305. doi: 10.1186/s12916-020-01749-w

54. Chen, CL, Hsu, SC, Ann, DK, Yen, Y, and Kung, HJ. Arginine signaling and cancer metabolism. *Cancers (Basel)*. (2021) 13:1–29. doi: 10.3390/cancers13143541

55. Parsamanesh, N, Asghari, A, Sardari, S, Tasbandi, A, Jamialahmadi, T, Xu, S, et al. Resveratrol and endothelial function: a literature review. *Pharmacol Res*. (2021) 170:105725. doi: 10.1016/j.phrs.2021.105725

56. Wu, Y, Ding, Y, Ramprasath, T, and Zou, MH. Oxidative stress, GTPCH1, and endothelial nitric oxide synthase uncoupling in hypertension. *Antioxid Redox Signal*. (2021) 34:750–64. doi: 10.1089/ars.2020.8112

57. Esposito, K, Marfella, R, Ciotola, M, Di Palo, C, Giugliano, F, Giugliano, G, et al. Effect of a mediterranean-style diet on endothelial dysfunction and markers of vascular inflammation in the metabolic syndrome: a randomized trial. *JAMA*. (2004) 292:1440–6. doi: 10.1001/jama.292.12.1440

58. Zhang, D, Chen, G, Manwani, D, Mortha, A, Xu, C, Faith, JJ, et al. Neutrophil ageing is regulated by the microbiome. *Nature*. (2015) 525:528–32. doi: 10.1038/nature15367

59. de Lange, KM, Moutsianas, L, Lee, JC, Lamb, CA, Luo, Y, Kennedy, NA, et al. Genome-wide association study implicates immune activation of multiple integrin genes in inflammatory bowel disease. *Nat Genet*. (2017) 49:256–61. doi: 10.1038/ng.3760

60. He, J, Song, Y, Li, G, Xiao, P, Liu, Y, Xue, Y, et al. Fbxw7 increases CCL2/7 in CX3CR1hi macrophages to promote intestinal inflammation. *J Clin Invest*. (2019) 129:3877–93. doi: 10.1172/JCI123374

61. Valatas, V, Kolios, G, and Bamias, G. TL1A (TNFSF15) and DR3 (TNFRSF25): a co-stimulatory system of cytokines with diverse functions in gut mucosal immunity. *Front Immunol*. (2019) 10:583. doi: 10.3389/fimmu.2019.00583

62. Yu, X, Wang, D, Wang, X, Sun, S, Zhang, Y, Wang, S, et al. CXCL12/CXCR4 promotes inflammation-driven colorectal cancer progression through activation of RhoA signaling by sponging miR-133a-3p. *J Exp Clin Cancer Res*. (2019) 38:32. doi: 10.1186/s13046-018-1014-x

63. Li, C, Zhang, S, Chen, X, Ji, J, Yang, W, Gui, T, et al. Farnesoid X receptor activation inhibits TGFBR1/TAK1-mediated vascular inflammation and calcification via miR-135a-5p. *Commun Biol*. (2020) 3:327. doi: 10.1038/s42003-020-1058-2

64. Saikumar Jayalatha, AK, Hesse, L, Ketelaar, ME, Koppelman, GH, and Nawijn, MC. The central role of IL-33/IL-1RL1 pathway in asthma: from pathogenesis to intervention. *Pharmacol Ther*. (2021) 225:107847. doi: 10.1016/j.pharmthera.2021.107847

65. Wang, Y, Li, B, and Zhao, Y. Inflammation in preeclampsia: genetic biomarkers, mechanisms, and therapeutic strategies. *Front Immunol*. (2022) 13:883404. doi: 10.3389/fimmu.2022.883404

66. Swan, C, Duroudier, NP, Campbell, E, Zaitoun, A, Hastings, M, Dukes, GE, et al. Identifying and testing candidate genetic polymorphisms in the irritable bowel syndrome (IBS): association with TNFSF15 and TNFalpha. *Gut*. (2013) 62:985–94. doi: 10.1136/gutjnl-2011-301213

67. Janssens, R, Struyf, S, and Proost, P. The unique structural and functional features of CXCL12. *Cell Mol Immunol*. (2018) 15:299–311. doi: 10.1038/cmi.2017.107

68. Yang, Q, Ren, GL, Wei, B, Jin, J, Huang, XR, Shao, W, et al. Conditional knockout of TGF-betaRII /Smad2 signals protects against acute renal injury by alleviating cell necroptosis, apoptosis and inflammation. *Theranostics*. (2019) 9:8277–93. doi: 10.7150/thno.35686

69. Bozza, MT, Lintomen, L, Kitoko, JZ, Paiva, CN, and Olsen, PC. The role of MIF on eosinophil biology and Eosinophilic inflammation. *Clin Rev Allergy Immunol*. (2020) 58:15–24. doi: 10.1007/s12016-019-08726-z

70. Markovic, I, and Savvides, SN. Modulation of signaling mediated by TSLP and IL-7 in inflammation, autoimmune diseases, and cancer. *Front Immunol*. (2020) 11:1557. doi: 10.3389/fimmu.2020.01557

71. Yu, GI, Song, DK, and Shin, DH. Associations of IL1RAP and IL1RL1 gene polymorphisms with obesity and inflammation mediators. *Inflamm Res*. (2020) 69:191–202. doi: 10.1007/s00011-019-01307-y

72. He, H, Del Duca, E, Diaz, A, Kim, HJ, Gay-Mimbrera, J, Zhang, N, et al. Mild atopic dermatitis lacks systemic inflammation and shows reduced nonlesional skin abnormalities. *J Allergy Clin Immunol*. (2021) 147:1369–80. doi: 10.1016/j.jaci.2020.08.041

73. Pancholy, SB, Bernat, IBertrand OF, and Patel, TM. Prevention of radial artery occlusion after transradial catheterization: the PROPHET-II randomized trial. *JACC Cardiovasc Interv*. (2016) 9:1992–9. doi: 10.1016/j.jcin.2016.07.020

74. Shi, G, Li, F, Zhang, L, Gong, C, Xue, S, Song, Y, et al. Retrograde recanalization of occluded radial artery: a single-centre experience and literature review. *J Endovasc Ther*. (2022) 29:755–62. doi: 10.1177/15266028211067732

75. Hirshfeld, JW Jr, and Nathan, AS. Deriving function from structure: applying Hagen-Poiseuille to coronary arteries. *JACC Cardiovasc Interv*. (2020) 13:498–501. doi: 10.1016/j.jcin.2019.11.031

76. Schiaffino, S, and Reggiani, C. Fiber types in mammalian skeletal muscles. *Physiol Rev*. (2011) 91:1447–531. doi: 10.1152/physrev.00031.2010